

ARTICLE

Physiologically-Based Pharmacokinetic Modeling of the Drug–Drug Interaction of the UGT Substrate Ertugliflozin Following Co-Administration with the UGT Inhibitor Mefenamic Acid

Ernesto Callegari^{1,*}, Jian Lin¹, Susanna Tse¹, Theunis C. Goosen¹ and Vaishali Sahasrabudhe²

The sodium-glucose cotransporter 2 inhibitor ertugliflozin is metabolized by the uridine 5'-diphospho-glucuronosyltransferase (UGT) isozymes UGT1A9 and UGT2B4/2B7. This analysis evaluated the drug–drug interaction (DDI) following co-administration of ertugliflozin with the UGT inhibitor mefenamic acid (MFA) using physiologically-based pharmacokinetic (PBPK) modeling. The ertugliflozin modeling assumptions and parameters were verified using clinical data from single-dose and multiple-dose studies of ertugliflozin in healthy volunteers, and the PBPK fraction metabolized assignments were consistent with human absorption, distribution, metabolism, and excretion results. The model for MFA was developed using clinical data, and *in vivo* UGT inhibitory constant values were estimated using the results from a clinical DDI study with MFA and dapagliflozin, a UGT1A9 and UGT2B4/2B7 substrate in the same chemical class as ertugliflozin. Using the verified compound files, PBPK modeling predicted an ertugliflozin ratio of area under the plasma concentration–time curves (AUC_R) of 1.51 when co-administered with MFA. ClinicalTrials.gov identifier: NCT00989079.

Study Highlights

WHAT IS THE CURRENT KNOWLEDGE ON THE TOPIC?

☑ Physiologically-based pharmacokinetic (PBPK) prediction of enzymatic drug–drug interactions (DDIs), especially in relation to cytochrome P450 (CYP) inhibition, has been increasingly used during drug development and in support of regulatory submissions. However, there are few examples of the use of PBPK modeling and simulation for evaluating DDIs due to uridine 5'-diphospho-glucuronosyltransferase (UGT) inhibition.

WHAT QUESTION DID THIS STUDY ADDRESS?

☑ What is the predicted DDI between ertugliflozin, UGT1A9 and UGT2B4/2B7 substrate, and the UGT inhibitor mefenamic acid (MFA) using PBPK modeling?

WHAT DOES THIS STUDY ADD TO OUR KNOWLEDGE?

☑ In this study, we utilized a novel approach by developing and verifying PBPK models for ertugliflozin and dapagliflozin, which have similar metabolic pathways, and leveraged the observed data from the MFA-dapagliflozin DDI study in order to predict the magnitude of the DDI between MFA and ertugliflozin.

HOW MIGHT THIS CHANGE DRUG DISCOVERY, DEVELOPMENT, AND/OR THERAPEUTICS?

☑ This approach would enable wider application of PBPK modeling of DDIs resulting from inhibition of non-CYP enzymatic pathways.

Ertugliflozin, an oral sodium-glucose cotransporter 2 (SGLT2) inhibitor, is approved in the United States¹ and European Union² for the treatment of adults with type 2 diabetes mellitus at daily doses of 5 or 15 mg, either as monotherapy or in combination with metformin or sitagliptin. In phase III, randomized, double-blind trials, ertugliflozin (alone or with metformin or sitagliptin) was associated with significant reductions in fasting plasma glucose, glycated hemoglobin, body weight, and blood pressure, and was well

tolerated.^{3–10} The pharmacokinetics (PKs) of ertugliflozin are similar in healthy subjects and patients with type 2 diabetes mellitus.¹¹ After oral administration, ertugliflozin is rapidly absorbed, with time to maximum concentration (T_{max}) of 1 hour,¹² and exposure increases proportionally with dose over the range of 0.5–300 mg.^{13,14} The absolute bioavailability of ertugliflozin is ~ 100%¹⁵ and co-administration with food does not have a clinically meaningful impact on ertugliflozin PKs.¹⁶

¹Department of Medicine Design—Pharmacokinetics, Dynamics, and Metabolism, Pfizer Global Research and Development, Pfizer Inc., Groton, Connecticut, USA;

²Department of Clinical Pharmacology, Pfizer Global Research and Development, Pfizer Inc., Groton, Connecticut, USA. *Correspondence: Ernesto Callegari (ernesto.callegari@pfizer.com)

Received: June 23, 2020; accepted: November 12, 2020. doi:10.1002/psp4.12581

The absorption, distribution, metabolism, and excretion (ADME) of ertugliflozin was evaluated after oral administration of 25-mg ^{14}C -ertugliflozin.¹² The primary clearance mechanism is metabolism, mainly by glucuronidation (~ 86%) with oxidation playing a minor role (~ 12%)¹²; renal excretion of unchanged ertugliflozin is low (~ 2%).¹² The main enzyme responsible for the major glucuronidation pathway, as determined by *in vitro* reaction phenotyping studies,^{12,17,18} is the uridine 5'-diphospho-glucuronosyl-transferase (UGT) [Correction added on 21 January 2021, after first online publication: the abbreviation for (UGT) has been corrected to uridine 5'-diphospho-glucuronosyltransferase throughout the article.] isozyme UGT1A9 (81%), with a lesser contribution from UGT2B4/2B7 (19%), leading to two pharmacologically inactive glucuronide metabolites.¹² Metabolism of ertugliflozin via the minor oxidative pathway is mainly by the cytochrome P450 (CYP) isozyme CYP3A4 (85–100%), with minor contributions from CYP3A5 (0–10%) and CYP2C8 (0–4%).^{12,17} As oxidation is a minor pathway, clinically significant drug–drug interactions (DDIs) are not expected following co-administration of ertugliflozin with CYP inhibitors. However, given that metabolism by UGT1A9 is the major clearance pathway of ertugliflozin, the potential for DDIs after co-administration with a UGT1A9 inhibitor needs to be evaluated.

Historically, drug interactions with UGT inhibitors have been evaluated in clinical studies and typically result in a less than two-fold increase in substrate drug exposures.¹⁹ Two clinical studies have evaluated DDIs between UGT inhibitors and the UGT substrates canagliflozin and dapagliflozin, which are SGLT2 inhibitors in the same chemical class as ertugliflozin. Canagliflozin is mainly metabolized by glucuronidation via UGT1A9 and UGT2B4 with a minor contribution from oxidation.²⁰ Co-administration of canagliflozin with probenecid (UGT1A9 inhibitory constant (K_i) = 2,452 μM^{21} ; probenecid 500-mg twice-daily dose estimated unbound maximum steady-state concentration ($C_{\text{max,ss,u}}$) = 29 μM ; inhibitor concentration/ $K_i \approx 0.01$) led to a 21% increase in canagliflozin exposure.²² Dapagliflozin has physicochemical and ADME properties similar to ertugliflozin, with the primary route of elimination of dapagliflozin being metabolism by glucuronidation (88%), predominantly by UGT1A9 with minor contributions from UGT2B4/2B7, whereas oxidative metabolism (10%) and renal elimination of unchanged drug (2%) are minor.²³ Co-administration of dapagliflozin with mefenamic acid (MFA; UGT1A9 and UGT2B4/2B7 inhibitor) led to a 51% increase in dapagliflozin exposure (ratio of the area under the plasma concentration–time curves (AUC_R) = 1.51).²⁴

Recent publications from the US Food and Drug Administration (FDA),²⁵ the European Medicines Agency (EMA),²⁶ and a position paper from the International Consortium for Innovation and Quality in Pharmaceutical Development consisting of over 35 pharmaceutical companies²⁷ highlight the utility of physiologically-based pharmacokinetic (PBPK) modeling approaches and affirm the acceptability of PBPK simulations in regulatory reviews.^{28,29} Consequently, the number of FDA New Drug Applications and EMA Marketing Application Authorisations containing PBPK analyses has increased by > 20-fold since

2004, with > 50% of the models assessing enzyme-based DDIs particularly CYP-mediated DDIs.^{30,31} However, there are few published examples of PBPK modeling approaches to simulate UGT-mediated DDIs. A mirabegron PBPK model incorporated UGT2B7-mediated metabolism (~ 30%) and was applied to simulate DDIs with fluconazole (CYP3A4 and UGT2B7 inhibitor) and probenecid.³² PBPK modeling has also been used to simulate DDIs with the UGT substrate and inhibitor valproic acid,³³ and with a regimen of three antiviral drugs (ombitasvir, dasabuvir, and paritaprevir) that are known UGT1A1 inhibitors.³⁴ An *in vitro*–*in vivo* scaling approach for UGT metabolism data combined with PBPK modeling was used to successfully simulate a DDI between the antiretroviral drug zidovudine and fluconazole (UGT2B7 inhibitor).³⁵

In the current study, the DDI between ertugliflozin and the UGT1A9 inhibitor MFA was evaluated using PBPK modeling by leveraging available clinical DDI results between dapagliflozin and MFA. The PBPK models for ertugliflozin and dapagliflozin were developed and verified based on results from clinical and *in vitro* studies using a similar modeling approach. The MFA model was developed based on available clinical data for MFA, and verified by simulating the DDI following co-administration with dapagliflozin. The impact of MFA on the PK of ertugliflozin was then simulated at clinically relevant doses using the verified PBPK models within the commercial PBPK platform Simcyp.³⁶

METHODS

In vitro studies for dapagliflozin and MFA

In vitro dapagliflozin UGT reaction phenotyping studies, *in vitro* MFA plasma protein binding, and UGT inhibition studies were conducted to provide additional input parameters for the dapagliflozin and MFA PBPK models (**Supplementary Methods**).

PBPK modeling and simulation strategy

The modeling strategy involved the development of PBPK models for ertugliflozin, dapagliflozin, and MFA using available clinical PK (i.v./oral/ADME) and *in vitro* data. The models were then verified using observed results from the oral PK studies, and the *in vivo* MFA UGT K_i values were estimated using results from the clinical DDI between MFA and dapagliflozin. Last, the verified PBPK models were applied to simulate the DDI following co-administration of ertugliflozin and MFA.

PBPK modeling and simulation was conducted using Simcyp version 15, release 1 (Certara USA, Princeton, NJ). The simulations were performed in a virtual population library of healthy volunteers within Simcyp (Sim-Healthy Volunteers) using the same age range (18–55 years) and gender distribution (0–50% women) as the clinical studies included in the model development and verification. A summary of the trial designs for all simulations is listed in **Table S1**.

Development of PBPK models for ertugliflozin and dapagliflozin

The ADME properties of ertugliflozin and dapagliflozin are similar (**Figure 1**) and both PBPK models were developed using a middle-out approach.³⁷ The measured PK properties (i.v. clearance (CL_{iv}) and volume of distribution at

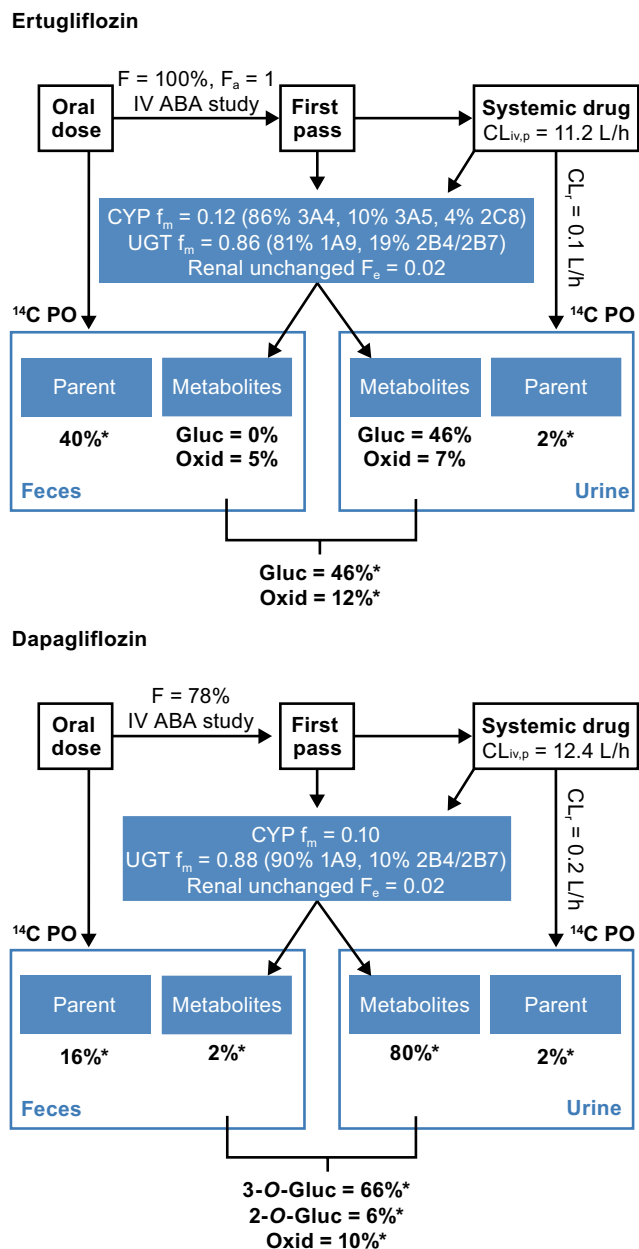


Figure 1 Flow chart showing ertugliflozin and dapagliflozin metabolism and disposition. See **Table S2** and **Table S3** for additional information on f_m assignments for ertugliflozin and dapagliflozin, respectively. Asterisk indicates values reported as % of dose; the identified parent, oxidative metabolites, and glucuronidation metabolites observed in feces and urine were scaled to 100% of the dose. ABA, absolute bioavailability; $CL_{iv,p}$, intravenous plasma clearance; CL_r , renal clearance; CYP, cytochrome P450; F, bioavailability; F_a , fraction absorbed; F_e , fraction excreted; f_m , fraction metabolized; Gluc, glucuronidation; Oxid, oxidation; UGT, uridine 5'-diphosphate-glucuronosyltransferase.

steady state (V_{ss}) after i.v. administration were used as input parameters during PBPK model development, and ADME results enabled the assignment of fraction metabolized (f_m) values due to glucuronidation or oxidation. The specific enzymatic clearance rates for ertugliflozin and

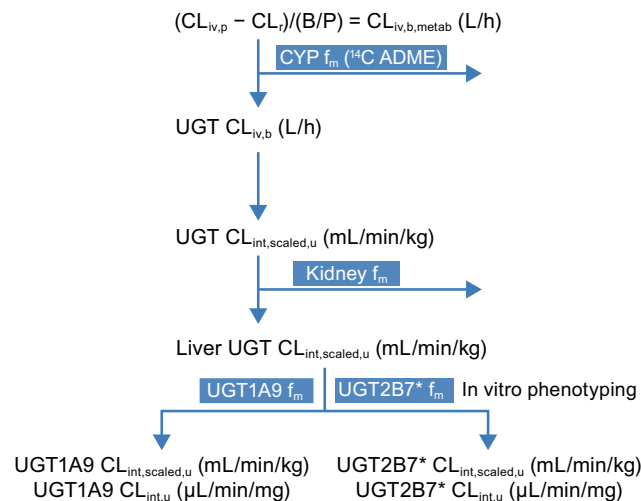


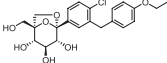
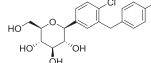
Figure 2 Flowchart showing the ertugliflozin and dapagliflozin elimination model development strategy. Asterisk indicates ertugliflozin and dapagliflozin metabolites by UGT2B4/2B7 was assigned to UGT2B7 in the PBPK model. ADME, absorption, distribution, metabolism, and excretion; B/P, blood/plasma ratio; CL_{int} , intrinsic clearance; $CL_{int,u}$, unbound intrinsic clearance; $CL_{iv,p}$, intravenous plasma clearance; $CL_{iv,b,metab}$, intravenous metabolic blood clearance; $CL_{iv,b}$, intravenous blood clearance; $CL_{int,scaled,u}$, unbound intrinsic clearance scaled; f_m , fraction metabolized; PBPK, physiologically-based pharmacokinetic; UGT, uridine 5'-diphospho-glucuronosyltransferase.

dapagliflozin were assigned using reaction phenotyping results and the approach defined in **Figure 2**. This approach was needed as the Retrograde Translation Tool in Simcyp version 15 did not incorporate metabolism by UGT enzymes.

Ertugliflozin model development. The ertugliflozin PBPK model was developed using clinical PK and *in vitro* data (**Table 1**). A minimal PBPK distribution model with the observed V_{ss} was used. Due to the biphasic i.v. PK profile, the volume of an additional single adjusting compartment (V_{sac}) [Correction added on 21 January 2021, after first online publication: the abbreviation for volume of an additional single adjusting compartment (V_{sac}) has been included.] and the first-order rate constants K_{in} and K_{out} were estimated in Simcyp using the parameter estimation module. For simulations after an oral dose, the first-order absorption model was used, with the fraction absorbed (F_a) value set to 1 based on results from the absolute bioavailability study.¹⁵ The coefficient of variation for F_a was set to 0% to capture the observed area under the plasma concentration–time curve (AUC). The human permeability coefficient was estimated from *in vitro* Caco-2 results, and absorption rate constant (K_a) values were estimated using sensitivity analysis to capture the maximum plasma concentration (C_{max}). An absorption lag time of 0.5 hours was estimated to match the observed T_{max} values.

The *in vivo* metabolism of ertugliflozin was characterized in the human ADME study following administration of a single oral dose of 25-mg ¹⁴[C]-ertugliflozin.¹² In this study, the measured renal clearance (CL_r) was low, with ~ 2% of the dose

Table 1 Simcyp input parameters for ertugliflozin, dapagliflozin, and MFA

Parameters	Ertugliflozin	Source	Dapagliflozin	Source	MFA	Source
Physicochemical properties						
Structure		Ref. 48		Ref. 23		Ref. 49
Molecular weight, g/mol	436	Ref. 42	408	DrugBank ⁵⁰	241	DrugBank ⁴⁹
LogP	2.5	Ref. 42	2.52	DrugBank ⁵⁰	5.4	DrugBank ⁴⁹
Compound type	Neutral	–	Neutral	–	Acid	–
pKa	–	–	–	–	3.89	DrugBank ⁴⁹
F _{u,plasma}	0.064	Ref. 45	0.09	Ref. 46	0.002	Measured (see Supplementary Information)
B/P ratio	0.66	Ref. 45	0.88	Ref. 46	1	Assumed
Absorption						
F _a	1.0	Ref. 15	0.9	Ref. 38	1.0	Assumed
K _a , h ⁻¹	1.2	Estimated (Simcyp) ^a	1.2	Estimated (Simcyp) ^a	0.85	Estimated (Simcyp) ^a
T _{lag} , hours	0.5	Estimated (Simcyp) ^a	–	–	–	–
Caco-2, 10 ⁻⁶ cm/s	4.1	Ref. 17	15.9	Ref. 46	–	–
Q _{gut} , L/h	5.62	Predicted (Simcyp)	8.5	Predicted (Simcyp)	–	–
Distribution						
V _{ss} , L/kg	1.23	Ref. 15	1.19	Ref. 38	0.4	Estimated (Simcyp) ^a
V _{sac} , L/kg	1.12	Estimated (Simcyp) ^a	0.9	Estimated (Simcyp) ^a	–	–
K _{in} , h ⁻¹	3.34	Estimated (Simcyp) ^a	–	–	–	–
K _{out} , h ⁻¹	0.56	Estimated (Simcyp) ^a	–	–	–	–
Q, L/h	–	–	10	Estimated (Simcyp) ^a	–	–
Elimination						
CL _{iv} , L/h	11.2	Ref. 15	12.4	Ref. 38	–	–
CL _r , L/h	0.1	Ref. 42	0.2	Ref. 23	–	–
CL _{int} , CYP, μL/min/pmol	CYP3A4 = 0.041 CYP3A5 = 0.006 CYP2C8 = 0.011	Retrospectively calculated based on: CL _{iv} (11.2 L/h) CL _r (0.1 L/h); CYP f _m (0.12) CYP3A4 (86%) CYP3A5 (10%) CYP2C8 (4%)	–	–	–	–
Additional HLM CL _{int} , μL/min/mg	–	–	4	Retrospectively calculated based on: CL _{iv} (12.4 L/h; Ref. 38) CL _r (0.2 L/h; Ref. 23) CYP f _m (0.10; Ref. 23)	–	–
CL _{int} , UGT, μL/min/mg	UGT1A9 = 35 UGT2B7 = 8	Calculated based on: UGT1A9 (81%) UGT2B7 (19%)	UGT1A9 = 30 UGT2B7 = 3	Calculated based on: UGT1A9 (90%) UGT2B7 (10%)	–	–

(Continues)

Table 1 (Continued)

Parameters	Ertugliflozin	Source	Dapagliflozin	Source	MFA	Source
CL _{po} , L/h	-	-	-	-	17	Estimated (Simcyp) ^a
K _i vs. UGT1A9, μM	-	-	-	-	0.038	Fitted based on clinical DDI ^b
K _i vs. UGT2B7, μM	-	-	-	-	0.051	Fitted based on clinical DDI ^b

B/P ratio, blood/plasma ratio; Caco-2, permeability coefficient; CL_{int}, intrinsic clearance; CL_{iv}, clearance observed for intravenous administration; CL_{po}, clearance observed for oral administration; CL_r, renal clearance; CYP, cytochrome P450; DDI, drug-drug interaction; F_a, fraction absorbed; f_m, fraction metabolized; F_{u,plasma}, fraction unbound in plasma; HLM, human liver microsomes; K_a, absorption rate constant; K_i, reversible inhibitory constant; K_{in}, first-order rate constant in; K_{out}, first-order rate constant out; LogP, partition coefficient; MFA, mefenamic acid; pKa, acid dissociation constant; Q, intercompartmental clearance; Q_{gut}, hybrid term including both villous blood flow and permeability through the enterocyte membrane; Ref., reference citation; T_{lag}, lag time; UGT, uridine 5'-diphospho-glucuronosyltransferase; V_{sac}, volume of single adjusting compartment; V_{ss}, volume of distribution at steady state; -, data not available or not applicable.

^aSimcyp parameter estimate.

^bK_i values were fitted to recover the observed clinical DDI between MFA and dapagliflozin.²⁴ Relative *in vitro* potency between UGT1A9 K_i = 0.11 μM and UGT2B7 K_i = 0.15 μM was maintained.

excreted unchanged (F_e = 0.02), and ~ 12% of ertugliflozin was converted to oxidative metabolites and assigned to CYP metabolism (f_{m,CYP} = 0.12). The remaining metabolism was assigned to glucuronidation (f_{m,UGT} = 0.86; **Table S2**).

The assignment of enzymatic clearance rates is defined in **Figure 2**. The Simcyp Retrograde Translation Tool was used to estimate intrinsic clearance (CL_{int}) values for ertugliflozin based on measured CL_{iv} and CL_r values. The f_{m,CYP} (0.12) from the ADME study and available ertugliflozin *in vitro* CYP reaction phenotyping results (CYP3A4 = 86%; CYP3A5 = 10%; and CYP2C8 = 4%) assigned f_m values for specific CYP enzymes (f_{m,CYP} × % contribution): f_{m,CYP3A4} = 0.103; f_{m,CYP3A5} = 0.012; and f_{m,CYP2C8} = 0.005. These f_m values were used to calculate the ertugliflozin CL_{int,CYP} values for each enzyme. The remaining CL_{int} was assigned to glucuronidation (UGT CL_{int,u}) and scaled to give a systemic enzymatic clearance (UGT CL_{int,scaled,u}). *In vitro* studies in human liver and kidney microsomes showed that 10% of the systemic ertugliflozin UGT clearance occurs in the kidneys, whereas 90% occurs in the liver.¹⁸ Thus, 10% of the UGT CL_{int,scaled,u} was subtracted and the remaining CL_{int,scaled,u} was assigned to liver UGTs. *In vitro* ertugliflozin UGT reaction phenotyping studies^{12,17,18} showed that the relative contribution of UGT1A9 was 81%, and the contribution of the UGT2B4/2B7 isozymes was 19%. For modeling purposes, the minor UGT contribution was assigned to UGT2B7. Therefore, an ertugliflozin UGT1A9 CL_{int,u} of 35 μL/min/mg and a UGT2B7 CL_{int,u} of 8 μL/min/mg were calculated and used as input parameters in the ertugliflozin compound file.

Dapagliflozin model development. The dapagliflozin PBPK model was developed using clinical and *in vitro* results, similar to the approach used for the ertugliflozin model (**Table 1**). A minimal PBPK distribution model was used. Due to the biphasic i.v. PK profile, parameters for V_{sac} and intercompartmental clearance were determined by fitting the i.v. PK profile³⁸ using the parameter estimation module in Simcyp. The first-order absorption model was used for fitting the oral data,³⁸ and the K_a was estimated using a sensitivity analysis in Simcyp. The F_a was estimated using the measured CL_{iv} (12.4 L/

hour) and bioavailability (78%) using the following relationship: $F = F_a \times F_g \times F_h$.³⁸ The dapagliflozin F_a was 0.9, where the fraction of drug remaining after first-pass through the intestinal wall (F_g) was assumed to be 1 due to low oxidative metabolism (F_a × F_g = 0.91). In the human ADME study, 10% of dapagliflozin was converted to oxidative metabolites (f_{m,CYP} = 0.10) and the measured CL_r of dapagliflozin was low, with 2% of the dose excreted unchanged (F_e = 0.02).²³ The remainder of dapagliflozin metabolism was assigned to glucuronidation (f_{m,UGT} = 0.88), as defined in **Figure 1** and **Table S3**; assignment of dapagliflozin enzymatic clearance rates is defined in **Figure 2**. Using the Simcyp Retrograde Translation Tool and assigning 10% to CYP metabolism, the dapagliflozin oxidative CL_{int} was estimated (CL_{int} = 4 μL/min/mg) and listed as human liver microsomal clearance. The remaining CL_{int} was assigned to glucuronidation (UGT CL_{int,u}) and scaled to give a systemic enzymatic clearance (UGT CL_{int,scaled,u}). Similar to ertugliflozin, 10% of the systemic dapagliflozin UGT clearance occurs in the kidneys, whereas 90% occurs in the liver.³⁹ Thus, 10% of the UGT CL_{int,scaled,u} was subtracted and the remaining CL_{int,scaled,u} was assigned to liver UGTs. *In vitro* UGT reaction phenotyping studies indicated that 90% of the dapagliflozin UGT metabolism was due to UGT1A9, and the remaining 10% of UGT metabolism was assigned to UGT2B7 (**Supplementary Methods; Supplementary Results**). Thus, a UGT1A9 CL_{int,scaled,u} of 30 μL/min/mg and a UGT2B7 CL_{int,scaled,u} of 3 μL/min/mg were the input parameters for the dapagliflozin compound file.

Development of a PBPK model for MFA

The PBPK model for MFA was developed using a top-down approach using clinical data⁴⁰; the input parameters are listed in **Table 1**. A minimal PBPK distribution model with first-order absorption was used and V_{ss}, K_a, and clearance values after oral administration were determined by fitting the clinical data to match the observed PK profile following a 500-mg dose of MFA. *In vitro* K_i values for MFA inhibition of UGT1A9 (0.11 μM) and UGT2B7 (0.15 μM) were the initial input parameters (**Supplementary Methods**;

Table 2 Predicted and observed geometric mean (%CV) PK parameters of ertugliflozin and dapagliflozin after single and multiple oral doses, and MFA after a single oral dose

Dose	Predicted C_{max} , ng/mL	Predicted AUC _{inf} , ng·h/mL	Observed C_{max} , ng/mL	Observed AUC _{inf} , ng·h/mL	C_{max} predicted/observed ratio	AUC predicted/observed ratio
Ertugliflozin: single dose						
0.1 mg ^{a,b}	8.46 (63)	9.19 (35)	8.51 (32)	8.48 (15)	0.98	1.08
15 mg ^a	249 (69)	1140 (50)	256 (14)	1400 (13)	0.97	0.81
0.5 mg	8.38 (64)	37.4 (44)	7.23 (11)	45.7 (10)	1.16	0.82
2.5 mg	41.9 (64)	187 (44)	42.8 (21)	231 (22)	0.98	0.81
10 mg	168 (64)	749 (44)	182 (22)	909 (15)	0.92	0.82
30 mg	503 (64)	2250 (44)	545 (24)	2810 (18)	0.92	0.80
100 mg	1680 (64)	7490 (44)	1620 (16)	9610 (16)	1.04	0.78
300 mg	4890 (66)	22000 (38)	4330 (20)	26400 (16)	1.13	0.83
Ertugliflozin: multiple dose ^c						
5 mg	99.3 (61)	410 (47) ^d	81.3 (29)	398 (18) ^d	1.22	1.03
15 mg	279 (61)	1160 (47) ^d	268 (20)	1190 (22) ^d	1.04	0.97
Dapagliflozin: single dose						
10 mg ^a	124	580	143	628	0.87	0.92
Dapagliflozin: multiple dose						
10 mg	123	537 ^d	119	506 ^d	1.03	1.06
50 mg	614	2690 ^d	728	2540 ^d	0.84	1.06
MFA: single dose						
500 mg ^e	6370	30400	6900	34200	0.92	0.89

%CV, geometric coefficient of variation; AUC, area under the plasma concentration–time curve; AUC_{inf}, AUC from time 0 to infinity; C_{max} , maximum plasma concentration; K_a , absorption rate constant; MFA, mefenamic acid; PK, pharmacokinetic; V_{ss} , volume of distribution at steady-state.

^aModel development.

^bAdministered intravenously.

^cExposures at steady-state, following 6 days of single-dose administration.

^dAUC from time 0 to 24 hours postdose.

^ePK profile was used to estimate V_{ss} and K_a in Simcyp.

Supplementary Results) used to simulate the DDI following co-administration of MFA (500-mg loading dose then 250 mg every 6 hours for 4 days) with dapagliflozin (10-mg single dose on day 2). The DDI was underpredicted, thus the MFA *in vivo* UGT K_i values were optimized by fitting the clinical DDI data,²⁴ while keeping the relative potencies of UGT1A9 and UGT2B7 inhibition. The estimated *in vivo* MFA UGT1A9 and UGT2B7 K_i values were adjusted ~ 2.9-fold to 0.038 μ M and 0.051 μ M, respectively, and were used as input parameters for verification of the MFA compound file.

PBPK model verification

Ertugliflozin and dapagliflozin model verification. The ertugliflozin model was verified by comparing simulated plasma concentration–time profiles and PK results from single-dose (0.5–300 mg) and multiple-dose (5 mg and 15 mg) studies, where steady-state is achieved after 6 days of dosing, to observed clinical data.^{13,14,41,42} The dapagliflozin model was verified by comparing simulated plasma concentration–time profiles and PK results from multiple-dose studies (10 mg and 50 mg) to observed clinical data.⁴³ The ertugliflozin and dapagliflozin Simcyp-estimated f_m and F_e values were compared with observed results from the clinical ADME study and *in vitro* reaction phenotyping studies.

MFA model verification and *in vivo* UGT K_i values.

The MFA model was verified by comparison of the simulated plasma concentration–time profile and PK

results following a single 500-mg dose. The *in vivo* UGT K_i values were estimated by simulating DDI following co-administration of MFA (500-mg loading dose then 250 mg every 6 hours for 4 days) with dapagliflozin (10-mg single dose on day 2).

Simulation of co-administration of ertugliflozin and MFA

The co-administration of MFA (500-mg loading dose then 250 mg every 6 hours for 4 days) and ertugliflozin (15-mg single dose on day 2) was simulated to assess the impact of a UGT inhibitor on ertugliflozin PK.

RESULTS

In vitro studies for dapagliflozin and MFA

From the *in vitro* studies (see **Supplementary Results**), UGT1A9 (90%) was the primary enzyme involved in dapagliflozin glucuronidation. MFA inhibited UGT1A9 and UGT2B7 with unbound half-maximal inhibitory concentration/ K_i values of 0.22/0.11 and 0.30/0.15 μ M, respectively, but did not inhibit UGT2B4 *in vitro*. The MFA plasma unbound fraction was 0.0022.

Ertugliflozin and dapagliflozin PBPK model verification

The predicted and observed PK parameters of ertugliflozin and dapagliflozin following single (ertugliflozin 0.5–300-mg; dapagliflozin 10-mg) and multiple (ertugliflozin

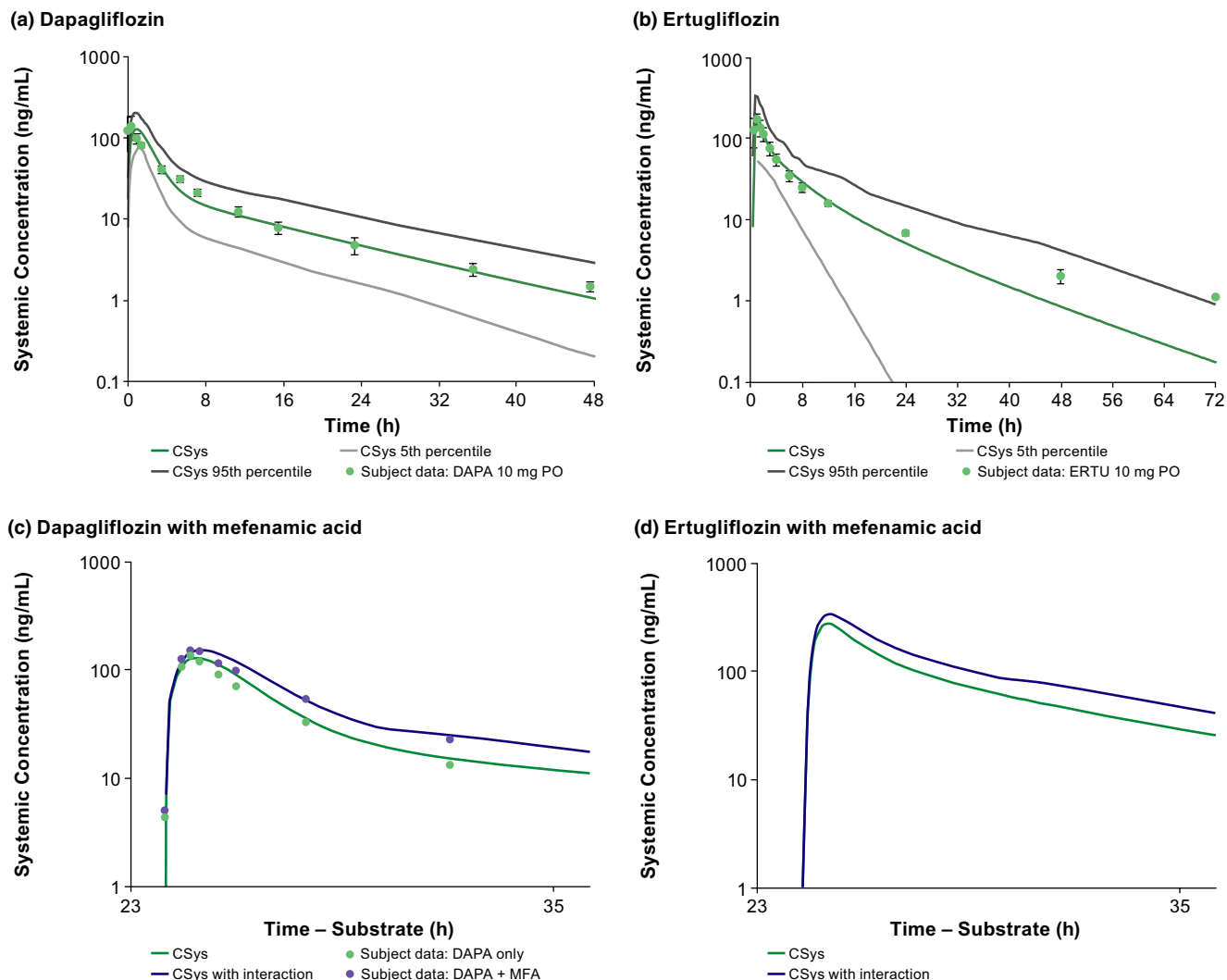


Figure 3 Clinically observed and PBPK model-predicted plasma concentrations of ertugliflozin and dapagliflozin in healthy subjects following single-dose oral administration with or without multiple-dose administration of MFA. (a) Dapagliflozin 10 mg, (b) ertugliflozin 10 mg, (c) dapagliflozin 10 mg (dosed on day 2) following MFA (500-mg loading dose and 250 mg every 6 hours for 4 days), and (d) ertugliflozin 15 mg (dosed on day 2) following MFA (500-mg loading dose and 250 mg every 6 hours for 4 days). The observed and predicted plasma concentrations were expressed as mean (green or purple circles) and mean (green or purple lines), respectively, with 5th and 95th percentiles shown (gray lines), in the control treatment (green) and following co-administration with MFA (purple). Where available, SD around the observed means are also shown (black whiskers). CSys, systemic concentration; DAPA, dapagliflozin; ERTU, ertugliflozin; MFA, mefenamic acid; PBPK, physiologically based pharmacokinetic; PO, prescribed orally.

5-mg and 15-mg; dapagliflozin 10-mg and 50-mg) oral doses^{13,14,41-43} are in **Table 2**. The predicted plasma vs. time profiles of dapagliflozin and ertugliflozin are shown in **Figure 3a,b**, respectively, for the single 10-mg dose, and in **Figures S1-S3** for the other dose regimens. The predicted plasma profiles after oral dosing are comparable to the observed clinical data for ertugliflozin and dapagliflozin. After single-dose and multiple-dose administration of ertugliflozin or dapagliflozin, the C_{max} predicted/observed ratios were within 80–125% of observed values. The ertugliflozin AUC predicted/observed ratios were within 77–84% of observed after a single dose and within 80–125% after multiple doses across the dose range of 0.5–300 mg. The dapagliflozin AUC predicted/observed

ratios were within 80–125% of observed values at all doses simulated.

The Simcyp-estimated ertugliflozin and dapagliflozin f_m and F_e values based on the input parameters were similar to the f_m and F_e values derived from ADME and disposition studies. For ertugliflozin, the estimated values were $f_{m,UGT1A9} = 0.71$, $f_{m,UGT2B7} = 0.17$, $f_{m,CYP3A4} = 0.10$, $f_{m,CYP3A5} = 0.002$, $f_{m,CYP2C8} = 0.01$, and urine $F_e = 0.01$; observed values were $f_{m,UGT1A9} = 0.70$, $f_{m,UGT2B7} = 0.16$, $f_{m,CYP3A4} = 0.103$, $f_{m,CYP3A5} = 0.012$, $f_{m,CYP2C8} = 0.005$, and urine $F_e = 0.02$ (**Figure S4**). For dapagliflozin, estimated values were $f_{m,UGT1A9} = 0.81$, $f_{m,UGT2B7} = 0.076$, $f_{m,CYP} = 0.094$, and urine $F_e = 0.018$; observed values were $f_{m,UGT1A9} = 0.79$, $f_{m,UGT2B7} = 0.09$, $f_{m,CYP} = 0.10$, and

Table 3 Predicted and observed geometric mean ratios (CI^a) for AUC (AUC_R) and C_{max} (C_{maxR}) following co-administration of dapagliflozin or ertugliflozin with MFA

	AUC _R	C _{maxR}
Dapagliflozin		
Predicted	1.53 (1.50–1.55)	1.18 (1.17–1.19)
Observed ^b	1.51 (1.44–1.58)	1.13 (1.03–1.24)
Predicted/observed ratio	1.0	1.0
Ertugliflozin		
Predicted	1.51 (1.48–1.54)	1.19 (1.17–1.20)

AUC_{inf}, area under the plasma concentration–time curve from time 0 to infinity; AUC_R, ratio of AUC_{inf} of substrate drug with co-administration of the interacting drug to AUC_{inf} of substrate drug alone; CI, confidence interval; C_{max}, maximum plasma concentration; C_{maxR}, ratio of C_{max} of substrate drug with co-administration of the interacting drug to C_{max} of the substrate drug alone; DDI, drug–drug interaction; K_i, inhibitory constant; MFA, mefenamic acid.

^aPredicted ratios show a 95% CI; observed ratios show a 90% CI.

^bResults from a clinical DDI study between dapagliflozin and MFA were used to fit the *in vivo* MFA K_i values.

urine $F_e = 0.02$ (Figure S5). For ertugliflozin, the Simcyp-estimated kidney UGT clearance was 14%, which was similar to the initial estimation of 10%. These simulation results provided confirmation of the absorption, distribution, $f_{m,UGT}$, $f_{m,CYP}$, and F_e assignments of the ertugliflozin and dapagliflozin PBPK models.

MFA PBPK model verification and *in vivo* UGT K_i values

The predicted and observed PK parameters of MFA following a 500-mg single oral dose are listed in Table 2, and the plasma PK profile is shown in Figure S6. The C_{max} and AUC predicted/observed ratios were within 80–125% of observed values. The simulation results provided verification of the observed MFA PK profile.

The MFA PBPK model was evaluated by simulation of the DDI with dapagliflozin using the verified dapagliflozin PBPK model, and using the optimized K_i values for UGT1A9 (0.038 μM) and UGT2B7 (0.051 μM) obtained by fitting the *in vivo* data. The predicted and observed PK parameters are in Table 3, and dapagliflozin plasma profiles in the absence or presence of MFA are shown in Figure 3c. Using the optimized MFA PBPK model, the predicted PK impact of MFA on dapagliflozin (AUC_R = 1.53; C_{maxR} = 1.18) recapitulated the observed values (AUC_R = 1.51; C_{maxR} = 1.13).

Simulation of ertugliflozin PK following co-administration with MFA

Using the verified ertugliflozin and MFA PBPK models, the DDI following co-administration of ertugliflozin and MFA was simulated. Results are summarized in Table 3, and the simulated PK profiles in the absence or presence of MFA are shown in Figure 3d. The predicted ertugliflozin AUC_R value was 1.51 and the C_{maxR} value was 1.19 in the presence of the UGT inhibitor MFA.

A sensitivity analysis was conducted to evaluate the increase in UGT f_m (from 0.86 to 0.93) and decrease in CYP f_m (from 0.12 to 0.06) by assuming that the secondary metabolites undergo glucuronidation as the initial step in

metabolism, while maintaining the *in vitro* reaction phenotyping results. The simulated co-administration with MFA predicted an ertugliflozin AUC_R = 1.55 and C_{maxR} = 1.20, which was consistent with results using the verified ertugliflozin model.

DISCUSSION

PBPK modeling and simulation have shown utility in drug development as they support the complexity required to evaluate mechanistic questions that require an in-depth understanding of human physiology.⁴⁴ This analysis uses PBPK modeling to simulate the DDI following co-administration of ertugliflozin with the UGT inhibitor MFA. The key components in predicting UGT DDIs are the quantitative assessment of the UGT enzymes responsible for metabolism and the validation of *in vivo* UGT K_i values for inhibitors.

There are several areas of uncertainty when assigning the contribution of UGT metabolism, including hydrolysis of glucuronide metabolites in the gastrointestinal tract after biliary excretion, and occurrence of UGT metabolism in hepatic and extrahepatic tissues due to the expression of UGTs in various organs. In the case of ertugliflozin, ~ 46% of the dose was recovered in excreta as primary glucuronides following an oral dose in the human ADME study (Table S2),¹² suggesting that the $f_{m,UGT}$ was at least 0.46. Additionally, ~ 40% of unchanged drug was recovered in the feces after an oral dose (Figure 1; Table S2). The unchanged drug in feces may be due to unabsorbed drug, biliary or gastrointestinal secretion of ertugliflozin, or hydrolysis of the primary glucuronides back to the parent compound. However, the absolute bioavailability study indicated complete absorption of ertugliflozin,¹⁵ and *in vivo* studies in animals and *in vitro* studies in human hepatocytes were indicative of minimal biliary excretion of ertugliflozin.^{12,17,45} Although gastrointestinal secretion of drugs cannot be ruled out, a large proportion of the unchanged ertugliflozin in feces is likely due to hydrolysis of primary glucuronides, which would indicate a higher $f_{m,UGT}$ value. As a worst-case scenario for the estimation of the DDI due to UGT inhibition, all of the unchanged drug in feces was assumed to be formed due to hydrolysis of primary glucuronides. Therefore, an $f_{m,UGT}$ value of 0.86 was used for the ertugliflozin PBPK model.

UGTs are expressed in multiple organs—mainly the liver, kidneys, and gastrointestinal tract—and metabolism is dependent on the specific UGT isoform expressed in each tissue. Therefore, it is important to determine the UGT isoform involved in order to understand the relative contributions of hepatic vs. extrahepatic metabolism. *In vitro* reaction phenotyping studies showed that ertugliflozin is metabolized mainly by UGT1A9 (81%).^{12,17} The minor UGT enzymes were assigned based on studies with the UGT inhibitor 16β-phenyllongifolol, which was recently shown to be a nonselective inhibitor of both UGT2B4 and UGT2B7. As selective inhibitors of UGT2B4 and UGT2B7 are not available, the minor UGT enzymes are reported as UGT2B4/2B7 (19%).^{12,17,18} Because MFA inhibits UGT1A9 and UGT2B7, and not UGT2B4, the minor UGT responsible

for metabolism of ertugliflozin was assigned to UGT2B7 in the PBPK model. This assignment provides a conservative assessment of the DDI following co-administration of ertugliflozin with the UGT1A9/2B7 inhibitor MFA. These UGT enzymes are found in the liver and the kidneys; therefore, the compound is subject to metabolism in both organs. Differential metabolism in these two organs was accounted for in the PBPK models for ertugliflozin. UGT metabolism in the kidneys can be estimated by Simcyp, which accounts for differences in tissue blood flows and enzyme expression between the two organs, using liver UGT1A9 and UGT2B7 CL_{int} values. For ertugliflozin, the liver and kidney UGT CL_{int} values were estimated and incorporated into the PBPK model. The resulting f_m assignments from the Simcyp output were similar to the f_m assignments based on the ADME,¹² bioavailability,¹⁵ and *in vitro* reaction phenotyping data.^{17,18} Together, these results show that the liver is the main organ of clearance for ertugliflozin. The same approach was used for the assignment of f_m and CL_{int} values for dapagliflozin and the development of the dapagliflozin PBPK model was similar.

After derivation of the various input parameters, including assignment of enzymatic pathways and f_m and CL_{int} values for the ertugliflozin and dapagliflozin PBPK models, both models were verified through comparison of simulated results to available clinical data. The close concordance between the simulated outcome and observed data serves to confirm that the models adequately captured the metabolism and disposition characteristics of each compound.

The MFA compound file was developed using available clinical PK data, as a PBPK model was not available, and optimized with the results from a clinical DDI study with dapagliflozin.²⁴ Given the similarities in ADME between ertugliflozin and dapagliflozin, the clinical DDI study results between MFA and dapagliflozin were critical to confirming the MFA UGT K_i values. The initial MFA model predicted the PK of MFA, but it could not be further verified due to lack of published PK and clinical DDI data for MFA. The initial model underestimated the observed DDI following co-administration of dapagliflozin and MFA when using the experimentally determined UGT1A9 and UGT2B7 K_i values. Therefore, the UGT1A9 and UGT2B7 K_i values were optimized (increased potency ~ 2.9-fold) using the clinical DDI data such that the predicted AUC_R and C_{maxR} matched the observed values as reported in the literature.

Given the similarities in ADME and bioavailability between ertugliflozin and dapagliflozin,^{12,15,17,23,38,46} the verified MFA PBPK model with optimized UGT K_i values was used to simulate the DDI following co-administration with the UGT substrate ertugliflozin. The PBPK model predicted an AUC_R of 1.51 and a C_{maxR} of 1.19 for the interaction between ertugliflozin and MFA. The magnitude of the predicted interaction is similar to the clinical DDI observed between MFA and dapagliflozin ($AUC_R = 1.51$; $C_{maxR} = 1.13$).²⁴

The safety and tolerability of ertugliflozin have been extensively studied throughout the drug's clinical development program. In phase I and II studies, single doses of ertugliflozin of up to 300 mg, and multiple daily doses of up to 100 mg for ≤ 14 days and up to 25 mg for ≤ 12 weeks, had an

acceptable safety profile.⁴² In phase III studies, ertugliflozin was safe and well-tolerated at both the 5-mg and 15-mg approved doses, with a safety profile that is generally consistent with other members of the SGLT2-inhibitor class.^{10,47} Based on the overall safety profile of ertugliflozin across a wide dose range and variety of patient populations, combined with the AUC_R of 1.51 for the predicted DDI between ertugliflozin and MFA from PBPK modeling, dose adjustment for safety reasons is not necessary when ertugliflozin is co-administered with MFA or other UGT1A9 and UGT2B7 inhibitors of similar potency. The predicted magnitude of the DDI was within the ertugliflozin concentration range with established safety data and supports the justification that a clinical DDI study with a UGT inhibitor or ertugliflozin dose adjustment was not necessary. The use of PBPK modeling and simulation using well-developed and verified compound models, as demonstrated in this study, contributes to improved efficiency and streamlining of drug development.

Supporting Information. Supplementary information accompanies this paper on the *CPT: Pharmacometrics & Systems Pharmacology* website (www.psp-journal.com).

Acknowledgments. The authors thank Kim Lapham, Jonathan Novak, and Nicholas Ferguson for the design and conduct of *in vitro* MFA UGT DDI studies.

Funding. This study was sponsored by Pfizer Inc., New York, NY, USA in collaboration with Merck Sharp & Dohme Corp., a subsidiary of Merck & Co., Inc., Kenilworth, NJ, USA. Editorial support was provided by Shirley Smith, PhD, of Engage Scientific Solutions (Horsham, UK) and was funded by Pfizer Inc., New York, NY, USA in collaboration with Merck Sharp & Dohme Corp., a subsidiary of Merck & Co., Inc., Kenilworth, NJ, USA.

Conflict of Interest. E.C., J.L., S.T., T.C.G., and V.S. are employees of Pfizer Inc., New York, NY, USA and may own shares/stock options in Pfizer Inc., New York, NY, USA.

Author Contributions. E.C., J.L., S.T., T.C.G., and V.S. wrote the manuscript. E.C., J.L., S.T., T.C.G., and V.S. designed the research. E.C. and J.L. performed the research. E.C., J.L., S.T., T.C.G., and V.S. analyzed the data.

Data-sharing Statement. Upon request, and subject to review, Pfizer will provide the data that support the findings of this study. Subject to certain criteria, conditions, and exceptions, Pfizer may also provide access to the related individual anonymized participant data. See <https://www.pfizer.com/science/clinical-trials/trial-data-and-results> for more information.

1. US Food and Drug Administration; Merck Sharp & Dohme Corp., a subsidiary of Merck & Co., Inc., Steglatro™ (ertugliflozin): Prescribing information <<https://www.accessdata.fda.gov/scripts/cder/daf/index.cfm?event=overview.proceedings&applno=209803>> (2017). Accessed May 13, 2020.
2. European Medicines Agency; Merck Sharp & Dohme Corp., a subsidiary of Merck & Co., Inc. Steglatro™ (ertugliflozin): Summary of product characteristics <<https://www.ema.europa.eu/en/medicines/human/EPAR/steglatro>> (2018). Accessed May 13, 2020.
3. Aronson, R. *et al.* Long-term efficacy and safety of ertugliflozin monotherapy in patients with inadequately controlled T2DM despite diet and exercise: VERTIS MONO extension study. *Diabetes Obes. Metab.* **20**, 1453–1460 (2018).
4. Miller, S. *et al.* Ertugliflozin and sitagliptin co-initiation in patients with type 2 diabetes: the VERTIS SITA randomized study. *Diabetes Ther.* **9**, 253–268 (2018).

5. Dagogo-Jack, S. *et al.* Efficacy and safety of the addition of ertugliflozin in patients with type 2 diabetes mellitus inadequately controlled with metformin and sitagliptin: the VERTIS SITA2 placebo-controlled randomized study. *Diabetes Obes. Metab.* **20**, 530–540 (2018).
6. Grunberger, G. *et al.* Ertugliflozin in patients with stage 3 chronic kidney disease and type 2 diabetes mellitus: the VERTIS RENAL randomized study. *Diabetes Ther.* **9**, 49–66 (2018).
7. Pratley, R.E. *et al.* Ertugliflozin plus sitagliptin versus either individual agent over 52 weeks in patients with type 2 diabetes mellitus inadequately controlled with metformin: the VERTIS FACTORIAL randomized trial. *Diabetes Obes. Metab.* **20**, 1111–1120 (2018).
8. Gallo, S. *et al.* Long-term efficacy and safety of ertugliflozin in patients with type 2 diabetes mellitus inadequately controlled with metformin monotherapy: 104-week VERTIS MET trial. *Diabetes Obes. Metab.* **21**, 1027–1036 (2019).
9. Hollander, P. *et al.* Results of VERTIS SU extension study: safety and efficacy of ertugliflozin treatment over 104 weeks compared to glimepiride in patients with type 2 diabetes mellitus inadequately controlled on metformin. *Curr. Med. Res. Opin.* **35**, 1335–1343 (2019).
10. Patel, S. *et al.* Safety of ertugliflozin in patients with type 2 diabetes mellitus: pooled analysis of seven phase 3 randomized controlled trials. *Diabetes Ther.* **11**, 1347–1367 (2020).
11. Sahasrabudhe, V. *et al.* The effect of renal impairment on the pharmacokinetics and pharmacodynamics of ertugliflozin in subjects with type 2 diabetes mellitus. *J. Clin. Pharmacol.* **57**, 1432–1443 (2017).
12. Miao, Z. *et al.* Pharmacokinetics, metabolism, and excretion of the antidiabetic agent ertugliflozin (PF-04971729) in healthy male subjects. *Drug Metab. Dispos.* **41**, 445–456 (2013).
13. Nucci, G., Le, V., Sweeney, K. & Amin, N. Single- and multiple-dose pharmacokinetics and pharmacodynamics of ertugliflozin, an oral selective inhibitor of SGLT2, in healthy subjects. *Clin. Pharmacol. Ther.* **103**, S83 (2018).
14. Fediuk, D.J. *et al.* Overview of the clinical pharmacology of ertugliflozin, a novel sodium-glucose cotransporter 2 (SGLT2) inhibitor. *Clin. Pharmacokinet.* **59**, 949–965 (2020).
15. Raje, S. *et al.* Novel application of the two-period microtracer approach to determine absolute oral bioavailability and fraction absorbed of ertugliflozin. *Clin. Transl. Sci.* **11**, 405–411 (2018).
16. Sahasrabudhe, V. *et al.* Effect of food on the pharmacokinetics of ertugliflozin and its fixed-dose combinations ertugliflozin/sitagliptin and ertugliflozin/metformin. *Clin. Pharmacol. Drug Dev.* **8**, 619–627 (2019).
17. Kalgutkar, A.S. *et al.* Preclinical species and human disposition of PF-04971729, a selective inhibitor of the sodium-dependent glucose cotransporter 2 and clinical candidate for the treatment of type 2 diabetes mellitus. *Drug Metab. Dispos.* **39**, 1609–1619 (2011).
18. Lapham, K. *et al.* *In vitro* characterization of ertugliflozin metabolism by UDP-glucuronosyltransferase and cytochrome P450 enzymes. *Drug Metab. Dispos.* **48**, 1350–1363 (2020). [Correction added on 21 January 2021, after first online publication: Reference 18 has been corrected.]
19. Williams, J.A. *et al.* Drug-drug interactions for UDP-glucuronosyltransferase substrates: a pharmacokinetic explanation for typically observed low exposure (AUC/AUC) ratios. *Drug Metab. Dispos.* **32**, 1201–1208 (2004).
20. Mamidi, R.N. *et al.* Metabolism and excretion of canagliflozin in mice, rats, dogs, and humans. *Drug Metab. Dispos.* **42**, 903–916 (2014).
21. Uchaipichat, V. *et al.* Human UDP-glucuronosyltransferases: isoform selectivity and kinetics of 4-methylumbelliferone and 1-naphthol glucuronidation, effects of organic solvents, and inhibition by diclofenac and probenecid. *Drug Metab. Dispos.* **32**, 413–423 (2004).
22. Devineni, D. & Polidori, D. Clinical pharmacokinetic, pharmacodynamic, and drug-drug interaction profile of canagliflozin, a sodium-glucose co-transporter 2 inhibitor. *Clin. Pharmacokinet.* **54**, 1027–1041 (2015).
23. Kasichayanula, S., Liu, X., Lacreata, F., Griffen, S.C. & Boulton, D.W. Clinical pharmacokinetics and pharmacodynamics of dapagliflozin, a selective inhibitor of sodium-glucose co-transporter type 2. *Clin. Pharmacokinet.* **53**, 17–27 (2014).
24. Kasichayanula, S., Liu, X., Griffen, S.C., Lacreata, F.P. & Boulton, D.W. Effects of rifampin and mefenamic acid on the pharmacokinetics and pharmacodynamics of dapagliflozin. *Diabetes Obes. Metab.* **15**, 280–283 (2013).
25. US Food & Drug Administration. Physiologically based pharmacokinetic analyses — format and content. Guidance for industry <<https://www.fda.gov/media/101469/download>> (2018). Accessed July 30, 2019.
26. European Medicines Agency. Guideline on the reporting of physiologically based pharmacokinetic (PBPK) modelling and simulation <https://www.ema.europa.eu/en/documents/scientific-guideline/guideline-reporting-physiologically-based-pharmacokinetic-pbpb-modelling-simulation_en.pdf> (2018). Accessed July 30, 2019.
27. Jones, H.M. *et al.* Physiologically based pharmacokinetic modeling in drug discovery and development: a pharmaceutical industry perspective. *Clin. Pharmacol. Ther.* **97**, 247–262 (2015).
28. Sinha, V., Zhao, P., Huang, S.M. & Zineh, I. Physiologically based pharmacokinetic modeling: from regulatory science to regulatory policy. *Clin. Pharmacol. Ther.* **95**, 478–480 (2014).
29. Zhao, P. *et al.* Applications of physiologically based pharmacokinetic (PBPK) modeling and simulation during regulatory review. *Clin. Pharmacol. Ther.* **89**, 259–267 (2011).
30. Grimstein, M. *et al.* Physiologically based pharmacokinetic modeling in regulatory science: an update from the U.S. Food and Drug Administration's Office of Clinical Pharmacology. *J. Pharm. Sci.* **108**, 21–25 (2019).
31. Luzon, E. *et al.* Physiologically based pharmacokinetic modeling in regulatory decision-making at the European Medicines Agency. *Clin. Pharmacol. Ther.* **102**, 98–105 (2017).
32. Konishi, K., Minematsu, T., Nagasaka, Y. & Tabata, K. Physiologically-based pharmacokinetic modeling for mirabegron: a multi-elimination pathway mediated by cytochrome P450 3A4, uridine 5'-diphosphate-glucuronosyltransferase 2B7, and butyrylcholinesterase. *Xenobiotica* **49**, 912–921 (2019).
33. Conner, T.M. *et al.* Physiologically based pharmacokinetic modeling of disposition and drug-drug interactions for valproic acid and divalproex. *Eur. J. Pharm. Sci.* **111**, 465–481 (2018).
34. Shebley, M. *et al.* Mechanisms and predictions of drug-drug interactions of the hepatitis c virus three direct-acting antiviral regimen: paritaprevir/ritonavir, ombitasvir, and dasabuvir. *Drug Metab. Dispos.* **45**, 755–764 (2017).
35. Crewe, H.K., Barter, Z.E., Humphries, H.E., Almond, L.M. & Rowland-Yeo, K. Application of physiologically based pharmacokinetic modelling to predict the pharmacokinetics of zidovudine and its interaction with fluconazole using recombinant UGT2B7 CL_{int} inputs and UGT tissue scalars. Drug Metabolism Discussion Group on Extra Hepatic Metabolism; Dundee, Scotland, UK: June 3–4, 2013.
36. Jamei, M. *et al.* The Simcyp population based simulator: architecture, implementation, and quality assurance. In *Silico Pharmacol.* **1**, 9 (2013).
37. Shebley, M. *et al.* Physiologically based pharmacokinetic model qualification and reporting procedures for regulatory submissions: a consortium perspective. *Clin. Pharmacol. Ther.* **104**, 88–110 (2018).
38. Boulton, D.W. *et al.* Simultaneous oral therapeutic and intravenous ¹⁴C-microdoses to determine the absolute oral bioavailability of saxagliptin and dapagliflozin. *Br. J. Clin. Pharmacol.* **75**, 763–768 (2013).
39. Kasichayanula, S. *et al.* The influence of kidney function on dapagliflozin exposure, metabolism and pharmacodynamics in healthy subjects and in patients with type 2 diabetes mellitus. *Br. J. Clin. Pharmacol.* **76**, 432–444 (2013).
40. Neuvonen, P.J. & Kivisto, K.T. Effect of magnesium hydroxide on the absorption of tolfenamic and mefenamic acids. *Eur. J. Clin. Pharmacol.* **35**, 495–501 (1988).
41. Dawra, V.K. *et al.* A PK/PD study comparing twice-daily to once-daily dosing regimens of ertugliflozin in healthy subjects. *Int. J. Clin. Pharmacol. Ther.* **57**, 207–216 (2019).
42. US Food & Drug Administration. Steglatro™ (ertugliflozin): Clinical pharmacology and biopharmaceutics review <https://www.accessdata.fda.gov/drugsatfda_docs/nda/2017/209803.209805.209806Orig1s000ClinPharmR.pdf> (2016). Accessed May 13, 2020.
43. Komoroski, B. *et al.* Dapagliflozin, a novel SGLT2 inhibitor, induces dose-dependent glucosuria in healthy subjects. *Clin. Pharmacol. Ther.* **85**, 520–526 (2009).
44. Wang, Y. & Huang, S.M. Commentary on fit-for-purpose models for regulatory applications. *J. Pharm. Sci.* **108**, 18–20 (2019).
45. US Food & Drug Administration. Steglatro™ (ertugliflozin): Non-clinical review <https://www.accessdata.fda.gov/drugsatfda_docs/nda/2017/209803.209805.209806Orig1s000PharmR.pdf> (2016). Accessed May 13, 2020.
46. Obermeier, M. *et al.* *In vitro* characterization and pharmacokinetics of dapagliflozin (BMS-512148), a potent sodium-glucose cotransporter type II inhibitor, in animals and humans. *Drug Metab. Dispos.* **38**, 405–414 (2010).
47. US Food & Drug Administration. Steglatro™ (ertugliflozin): Clinical review <https://www.accessdata.fda.gov/drugsatfda_docs/nda/2017/209803.209805.209806Orig1s000MedR.pdf> (2016). Accessed May 13, 2020.
48. Mascitti, V. *et al.* Discovery of a clinical candidate from the structurally unique dioxo-bicyclo[3.2.1]octane class of sodium-dependent glucose cotransporter 2 inhibitors. *J. Med. Chem.* **54**, 2952–2960 (2011).
49. DrugBank. Mefenamic acid <<https://www.drugbank.ca/drugs/DB00784>> (2019). Accessed May 13, 2020.
50. DrugBank. Dapagliflozin <<https://www.drugbank.ca/drugs/DB06292>> (2019). Accessed May 13, 2020.

© 2020 Pfizer Inc. *CPT: Pharmacometrics & Systems Pharmacology* published by Wiley Periodicals LLC on behalf of American Society for Clinical Pharmacology and Therapeutics. This is an open access article under the terms of the Creative Commons Attribution-NonCommercial-NoDerivs License, which permits use and distribution in any medium, provided the original work is properly cited, the use is non-commercial and no modifications or adaptations are made.